ACS OMEGA

Article

Cite This: ACS Omega 2018, 3, 18510−18517

http://pubs.acs.org/journal/acsodf

Structural and Mechanical Modification Induced by Water Content in Giant Wild Reed (*A. donax* L.)

Pellegrino Conte,*[,†] Vincenzo Fiore,[‡] and Antonino Valenza[‡]

[†]Dipartimento Scienze Agrarie, Alimentari e Forestali, v.le delle Scienze ed. 4, 90128 Palermo, Italy

[‡]Dipartimento Ingegneria Civile, Ambientale, Aerospaziale, dei Materiali, Università degli Studi di Palermo, v.le delle Scienze ed. 6, 90128 Palermo, Italy

ABSTRACT: Giant wild reed *Arundo donax* L. is an aggressive agricultural species with remarkable features such as fast-growing, untapped economic potential, eco-friendliness, and high specific properties (e.g., high strength/weight and modulus/weight ratios). Here, the bending properties of giant reed were studied at a molecular level to evaluate the effect of the conditions used during the preparation for their applications (also referred to as treatment conditions). The aim was to achieve new information potentially useful to suggest new possible applications of *A. donax* L. for structural applications in modern buildings. In this study, green reeds collected in a Sicilian plantation were dried for 2000 h in a climatic chamber under humidity−temperature-controlled conditions, then fully dried in an oven and finally re-moistened through two different procedures. The combination of different analytical techniques (such as calorimetry and fast field cycling NMR relaxometry) revealed that giant reed bending properties are strongly affected by the presence of bound water. In particular, it has been evidenced that a progressive enhancement of bending characteristics is obtained when the interactions between residual water and *A. donax* L. fibers become progressively stronger. For this reason, it can be suggested that fibers having different plasticity can be produced by modulate the heating treatment to regulate the amount of bound water inside *A. donax* L. fibers.

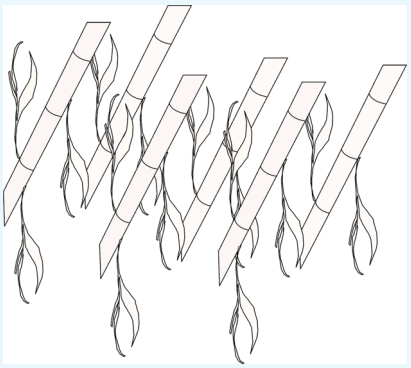

1. INTRODUCTION

An increasing interest for the use of natural materials for modern building exists in the current trend for sustainable development. In particular, renewable and natural resources, such as the giant reed *Arundo donax* L., can rapidly become source for inexpensive building materials in an increasingly eco-conscious world.

Giant reed is a perennial rhizomatous grass that grows plenty and naturally in all the temperate areas of Europe (mainly in the countries of the Mediterranean area such as Sicily, Italy) and can be easily adapted to different ecological conditions.[1] Due to its growing rate, it is an invasive, aggressive, and valueless species whose disposal is very difficult. For this reason, modern research aims at finding possible applications of the aforementioned costless giant reed to provide new and reliable materials to be used in eco-friendly applications. As an example, *A. donax* L. can be applied for the production of musical woodwind instruments[1] as a source of fibers for printing papers,[2,3] for drugs in medicinal applications,[4] as supporting material for composites,[5] or, in the latest years, as a source of biomass for chemical feedstock and for energy production.[6−8] Furthermore, this nonwood plant has been recently considered for the manufacturing of chipboard panels alternative to the wood-based ones,[9,10] as a source for both fibers[5] and particles[11,12] to be applied as reinforcement of polymer composites as well as to partially replace sand in concrete mixes.[13] The culm of giant reed is often used to make fences, trellises, stakes for plants, windbreaks, and sun shelters.[14] Owing to its high specific mechanical strength and modulus, the culms of giant reeds have been also employed in agricultural buildings, i.e., false ceilings, supports for roof cladding, and paneling of walls to improve their thermal performances up to the complete erection of both internal and external earthquake-resistant walls.[15]

Besides its specific properties, the attractive features of giant reed are the low density, the biodegradability, the recyclability, and the heterogeneous and efficient structure of the culm. The latter consists of two botanically distinct parts: nodes and internodes. The former stabilize and strengthen the entire culm versus the local buckling due to bending forces such as those due to the wind.[16,17] The mass proportion of nodes within the culm varies in the range 10−25%[18] depending on the length of the internodes which, in turn, varies between 10 and 30 cm.

Noteworthy, up to now, to the best of our knowledge, giant reed culms have been applied for the achievement of sustainable materials only in their natural conditions (that is, native wet and naturally or air-dried).[19−24] In particular, all the researches have been performed to achieve complete analyses of mechanical characteristics,[19,20] to study both viscoelastic[21] and dynamic[22] properties, and to evaluate the effects of drying

Received: October 4, 2018
Accepted: December 13, 2018
Published: December 27, 2018

DOI: 10.1021/acsomega.8b02649
ACS Omega 2018, 3, 18510−18517

treatments on the shrinkage characteristics.[23,24] None of the studies reported in literature is related to the influence of the conditions used to prepare the plant system for the production of building materials as affecting its bending properties.

The goal of this study relies on the achievement of wider giant reed bending properties by modulating the treatment conditions prior of any possible application in modern buildings. Green reeds were collected in a Sicilian plantation and dried under humidity−temperature-controlled conditions in a climatic chamber for a total duration of 2000 h. Then, the samples were oven-dried to remove the residual moisture content (MC) and finally re-moistened by means of two different procedures. Further, reeds dried through non-controlled conditions (i.e., naturally or air-dried) were investigated as a control. The investigations done by bending tests (Figure 1), calorimetry, and fast field cycling (FFC)

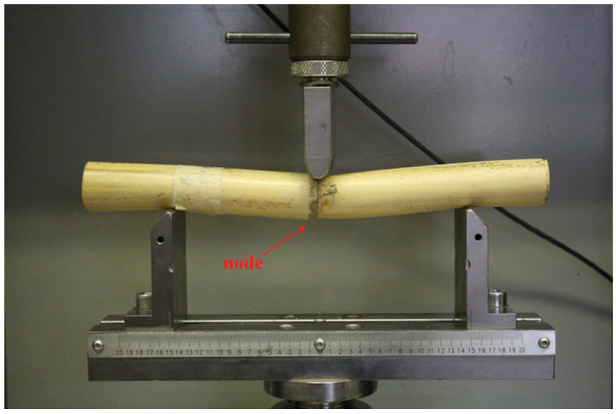

Figure 1. Configuration of bending test carried out on a sample with a node in their middle part (photo has been taken by one of the authors, V.F.).

nuclear magnetic resonance (NMR) relaxometry showed that controlling giant reed pretreatments result in a wider range of bending properties (in terms of rigidity, strength, and ductility) than those usually retrieved by applying the traditional conditions (i.e., naturally dried plant material).

2. RESULTS AND DISCUSSION

2.1. Moisture Content. The moisture content of all the *A. donax* L. samples (either with or without node) is reported in Figure 2 (refer to Table 1 for the meaning of the sample names used in the figure). Here, it is noticeable that the node-containing samples revealed a larger amount of water than the internodal ones (182 vs 146%, respectively). This can be explained by the presence of a larger amorphous cellulose fraction inside the nodes as compared with the internodes samples. Details about this explanation are given below when the calorimetric results will be accounted for.

A significant moisture content decrease occurs during the early 72 h of the controlled treatment. In particular, moisture content decreases from 181.8% (GREEN samples) to 51.7% (C-72 samples) for the node-containing samples; it goes from 146.1% (GREEN samples) to 13.9% (C-72 samples) for the nodeless samples.

At the end of the controlled treatment, the residual moisture contents of the C-2000 samples result 10.3 and 8.5% for node-containing and nodeless samples, respectively.

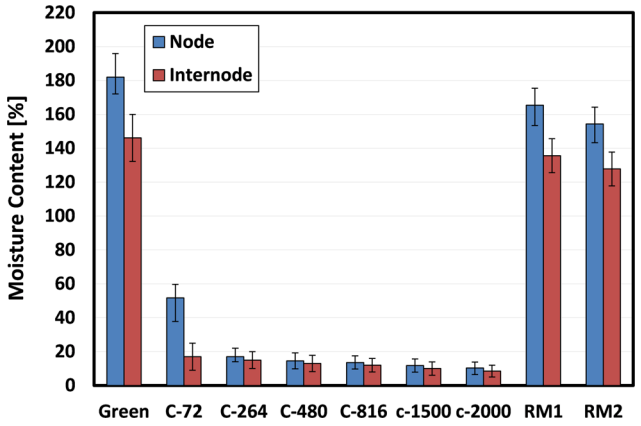

Figure 2. Moisture content as a function of the treatment conditions.

In the final phase of the controlled treatment, no notable changes are observed in the moisture content of the samples. For this reason, the residual moisture contents can be conceivably considered as the equilibrium moisture contents of the giant reed at the aforementioned conditions (i.e., temperature of 30 ± 2 °C and relative humidity (RH) of 50 ± 5%). Regardless of the presence of the node, the residual moisture contents of the UN samples (i.e., those naturally dried) are found to be 8.9%. As indicated above, these values can be considered as the equilibrium moisture contents of the reeds due to the natural drying treatment.

It is worth noting that the nodes appear to retard the drying phenomena of the giant reed in the first phase of the controlled treatment (i.e., in the time interval 0−24 h), as reported in literature.[24] In fact, the difference between the moisture contents of the samples with and without node increases up to 24 h of the controlled treatment. After this initial phase, the described difference decreases. Moreover, this difference is found larger than that measured (i.e., 35.6%) during the early 72 h of the treatment. At this drying duration, samples with and without node have lost similar amounts of moisture (i.e., 130.0 and 132.3%, respectively). After 72 h till the end of the control treatment, the difference between the moisture contents of the node-containing and nodeless samples is found to be lower than that measured for the GREEN samples. This means that, in this second phase of the controlled treatment, the drying process of the samples with node is faster than that of the samples without node.

The moisture content of the samples re-moistened in distilled water or in a 5% glucose solution increases till values are slightly lower than that of the GREEN samples. In particular, the moisture content of RM1 and RM2 samples with node is found to be 165.4 and 154.3%, respectively. The samples without node soaked in distilled water show an average moisture content of 135.6%, whereas those soaked in glucose solution of 127.8%.

2.2. Bending Stiffness. As previously reported, samples from naturally dried reeds were tested as it has been done for the control samples. Their bending properties are reported in Figure 3 (the samples are indicated with "UN" as indicated in Table 1). Because a node represents a thickening acting as a spring-like joint to support the culm by bending forces,[30] it can be hypothesized that node-containing samples reveal significantly stronger bending forces than the nodeless ones. In particular, the bending properties (both modulus and strength) of the samples with node increased by about 60% as compared

DOI: 10.1021/acsomega.8b02649
ACS Omega 2018, 3, 18510−18517

Table 1. Samples Tested in This Study and Their Designations

designation	treatment	time
UN	natural drying treatment	5 months
GREEN	NO (green reeds)	0 h
C-*X*	T = 30 ± 2 °C; RH = 50 ± 5%	*X* h[a]
DRY	T = 30 ± 2 °C; RH = 50 ± 5%	2500 h
	T = 103 ± 5 °C; RH = 50 ± 5%	24 h
RM1	T = 30 ± 2 °C; RH = 50 ± 5%	2500 h
	T = 103 ± 5 °C; RH = 50 ± 5%	24 h
	T = 25 ± 2 °C; immersion in distilled water	96 h
RM2	T = 30 ± 2 °C; RH = 50 ± 5%	2500 h
	T = 103 ± 5 °C; RH = 50 ± 5%	24 h
	T = 25 ± 2 °C; immersion in 5% glucose solution	96 h

[a]*X* indicates the number of hours of the control drying treatment in the time interval from 72 to 2000 h.

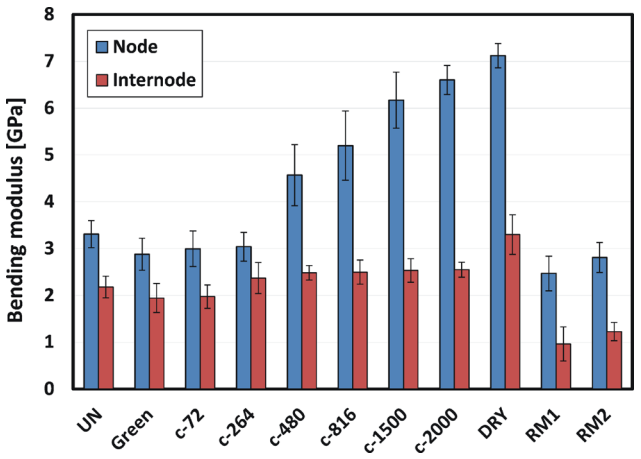

Figure 3. Variation of bending modulus as a function of the treatment conditions.

to the nodeless samples. As a consequence, the deformation at break of the UN samples without node (i.e., 2.49%) is 39% higher than the samples with node (i.e., 1.79%).

2.2.1. Node-Containing Samples. The variations of the bending modulus as a function of the treatment conditions are shown in Figure 3 (refer to Table 1 for the meaning of the sample names used in the figure). This figure shows that (1) the bending modulus remains almost constant in the first 264 h of the controlled drying treatment; (2) the bending modulus grows significantly after 264 h, showing a linear increase up to about 2000 h of the controlled treatment; (3) the bending modulus of the samples dried through the controlled method reaches the average value of the UN samples, after a treatment duration between 264 h (C-264) and 480 h (C-480); (4) the moisture-free samples (i.e., DRY) show a bending modulus of 148.3 and 109.7% larger than the GREEN samples and the UN samples, respectively; (5) the bending modulus of the samples re-moistened in distilled water (i.e., RM1 samples) is found to be 16 and 29% smaller than that of the GREEN samples and the UN samples, respectively; and (6) the bending modulus of the samples re-moistened in glucose solution (RM2) is found to be 3.5 and 18.5% lower than that of the GREEN samples and the UN samples, respectively.

As discussed above, the meaningful decrease of moisture content in the samples with node occurs in the early 72 h from the control drying treatment (i.e., from 181.8 to 51.7%).

Figure 3 also reveals that the bending stiffness improvements of the node-containing samples occur after 264 h from the control treatment (i.e., when the meaningful decrease of the moisture content has already occurred). This means that the aforementioned enhancements are not strictly connected to the meaningful decrease of moisture content but also to a different phenomenon occurring in the second time interval of the drying treatment. In fact, it is well recognized that the mechanical properties of wood and lignocellulosic materials are connected with the fiber saturation point (FSP).[31−35] The latter represents the moisture content of the cell cavities (i.e., the lumen) when they are completely devoid of free water (i.e., the water that is not bound neither chemically nor physically to the cell wall), whereas the cell walls are saturated with bound water (i.e., water bound to the cell wall via hydrogen bonds due to the presence of free hydroxyl groups in the cellulose, hemicelluloses, and lignin molecules). The importance of the FSP value relies on the fact that when the free-water/bound-water ratio is above FSP, free water accumulates in cell cavities.[36] As a consequence, the variations of moisture content have very little effect on the mechanical properties of wood and lignocellulosic materials. Conversely, as free-water/bound-water ratio is below the FSP value, the mechanical properties are strongly affected.

As reported in literature,[24] the FSP of *A. donax* L. giant reed is obtained when the moisture content is around 20% of the dry mass. By performing the control drying treatment (i.e., 30 ± 2 °C at RH of 50 ± 5%), the fiber saturation point is reached in the time interval between 72 and 264 h. For this reason, the increase in the bending properties after 264 h from the control treatment are due to the decrease in moisture content below the FSP.

The flexural modulus and the strength of the re-moistened samples are found to be lower than those of the GREEN samples because the drying treatment followed by the re-moistening procedure induces remarkable collapses of the parenchyma cells within the samples, as suggested in literature.[24]

2.2.2. Nodeless Samples. The influence of the treatment conditions on the bending stiffness is less evident in the nodeless samples as compared to the node-containing ones previously discussed. In particular, (1) the bending modulus of the samples mainly increases between 72 and 264 h of the controlled treatment; (2) after 264 h (C-264 samples) till the end of the control treatment (C-2000 samples), the bending modulus remains constant; (3) the DRY samples reveal a bending modulus that is 29% larger than that of C-2000, thereby suggesting that the elimination of the residual moisture within the samples at the end of the drying control treatment

DOI: 10.1021/acsomega.8b02649
ACS Omega 2018, 3, 18510−18517

(i.e., the equilibrium moisture content) brings an improvement of the bending stiffness of the giant reed; (4) at the end of the treatment, the samples referred to as C-2000 show bending modulus 30.9 and 19.5% larger than the GREEN and the UN samples, respectively; (5) the bending modulus of the nodeless samples reaches the average value found for the UN samples, after a duration of the control treatment between 72 and 264 h; (6) as in the previous case, the re-moistened nodeless samples reveal a bending modulus smaller than that of both the GREEN and UN samples; and (7) for the samples without node, it is possible to state that the FSP is reached in the first 72 h of the control treatment.

Due to the aforementioned discussion, it is possible to state that the increases of the bending stiffness after 72 h of the control treatment are due to the decrement of the moisture content below the FSP that, as reported previously, significantly influences the mechanical properties of lignocellulosic materials such as the giant reed.

2.3. Calorimetric Analysis. Figure 4 reports the DSC curves of the samples obtained from both the node and the internode of the GREEN reeds (refer to Table 1 for the name meaning). For both samples, an endothermic peak occurs at 140 °C due to the dehydration process of the lignocellulosic materials.[37−39]

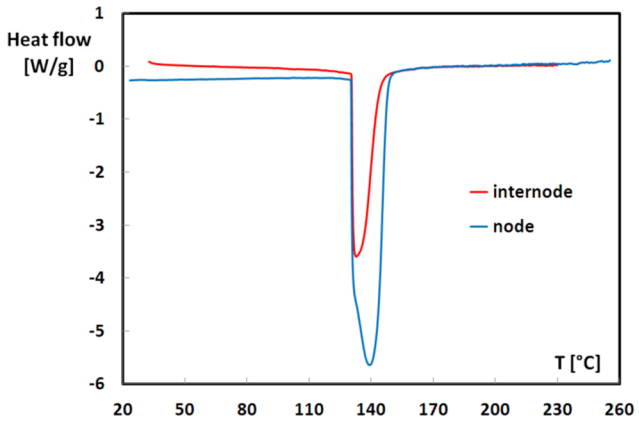

Figure 4. Di-endothermal processes recorded by differential scanning calorimetry (DSC) for the node and the internode of green reeds.

It is worth noting that the dehydration heat of the node is larger than that of the internode (Table 2).

Table 2. Dehydration Heats (in J g^{-1} of Total Weight) of Samples Obtained from the Node and from the Internode

designation	UN	GREEN	DRY	RM1	RM2
node	21.5	906.7	∼0	857.4	833.3
internode	13.6	416.2	∼0	345.8	324.3

It is usually recognized that water absorption occurs almost entirely in the amorphous regions of cellulose and in the entire volume of hemicellulose of lignocellulosic materials.[40] As both hemicelluloses and α cellulose contents do not differ significantly among the different morphological *A. donax* L. regions (i.e., nodes and internodes),[41] the area of the endothermic peak can be directly related to the amorphous fraction of cellulose.[42] In fact, as reported in Ciolacu et al.,[42] cellulose capability for water absorption depends largely on free hydroxyl groups availability. For this reason, water absorption occurs almost entirely in the amorphous regions of cellulose, thereby minimizing the role of the free hydroxyl groups that may be present on the surfaces of crystallites. Therefore, as water sorption occurs almost totally in the amorphous domain of cellulose, the area of the endothermic peak is directly related, due to the loss of absorbed water, to the amorphous fraction of cellulose. As a consequence, it can be concluded that the amorphous fraction of cellulose within node of giant reeds is larger than that within their intermodal zones.

Table 2 lists the dehydration heat values of the samples obtained from both the node and the internode, as a function of the treatment conditions. As expected, the dehydration heat decreases considerably with the increasing duration of the control treatment for both the analyzed samples. Nevertheless, residual values of the dehydration heat are measured till 1500 h of the control treatment. These residual heats of dehydration are strictly connected to the water bound to cell walls via hydrogen bonds (also referred to as bound water).

For what concerns the effect of the re-moistening procedures, the samples re-moistened in distilled water or in 5% glucose solution show heats of dehydration comparable to those of the GREEN samples, regardless of the presence of the node.

2.4. NMR Analysis. Longitudinal relaxation rates (R_1) of protons in liquid systems at the surface of porous media are affected by the collisions between the liquid-state molecules and the walls of the porous boundaries.[43] Weak interactions between the liquid-state molecules and the solid surfaces enable temporary adsorption,[44] thereby reducing the rotational tumbling rate. As a consequence, enhancement of $^1H-^1H$ dipolar interaction efficiency occurs and faster R_1 values are achieved.[27] However, the strength of the liquid−solid interactions and thus the efficiency of the proton relaxation is affected by pore size distribution. As matter of fact, water molecules laying in small-sized pores undergo space restrictions. Once this condition occurs, $^1H-^1H$ dipolar interactions become very efficient and faster relaxation rates are retrieved.[27] Conversely, increasing molecular mobility due to enhancement of pore sizes weakens the dipolar interactions so that slower relaxation rates are obtained.[27]

Water molecules form an infinite hydrogen-bonded network with localized and well-structured clustering that is usually referred to as "water structure". Once in the proximity of solid surfaces, water molecules interact with the surface functional groups through the formation of weak interactions such as ionic ones and H-bonds.[27] As a consequence, the overall three-dimensional water network is altered and two different possibilities may occur.[27] On the one hand, water molecules directly in contact with the solid surface may form strong interactions, thereby leading to a rigid ice-like shell, which is not flexible enough to sustain H-bonds among water molecules in that first hydration layer. The aforementioned strong interactions induce high polarization in water, thus favoring the formation of stronger hydrogen bonds with adjacent water molecules in the second hydration shell. As the distance from the solute increases, the effect of the interactions at the solid−liquid interface decreases and water molecules regain their normal behavior (i.e., they behave as a bulk). On the other hand, interactions among water molecules and solid surfaces may be weaker than in the aforementioned case and a less ice-like structured water is retrieved in the first layer. As a

DOI: 10.1021/acsomega.8b02649
ACS Omega 2018, 3, 18510−18517

consequence, H-bonds among water molecules in the different hydration layers are weaker than as previously described.

The strengthening effect on water structure as due to the strong interactions between solid surface and the first water layer is referred to as kosmotropic, whereas the effect due to the weak interactions is indicated as chaotropic.[27]

According to the mechanisms outlined above, the kosmotropic effect produces faster relaxation rates. Conversely, slower relaxation rates must be achieved as chaotropic conditions are fulfilled.[27]

Figure 5 reports the ^{1}H NMR dispersion (NMRD) profiles of the slow (Figure 5A) and fast (Figure 5B) relaxing components of water in contact with the fresh and dry plant materials (see Section 4). The two components refer to water molecules in the first (fast relaxing component) and the second (slow relaxing component) hydration layer around *A. donax* L. fibers, as described above. In both cases, the relaxation rates of the water molecules either in the first or in the second hydration shell resulted faster when interaction with the dry plant sample was accounted for (Figure 5). According to the mechanisms depicted above, we may argue that the fresh plant system revealed chaotropic properties, whereas the dry fibers resulted kosmotropic. The different behaviors can be explained by considering that the pores of the fresh sample are clogged by plant vascular water. The latter prevents exogenous water (i.e., the water used during the FFC NMR relaxometry experiments) to penetrate into pores, thereby leading the fresh plant fibers to chaotropic properties. Conversely, as plant fibers are desiccated (see Section 4), exogenous water flows into all the plant pores, thus revealing the kosmotropic effect of the dry plant system.

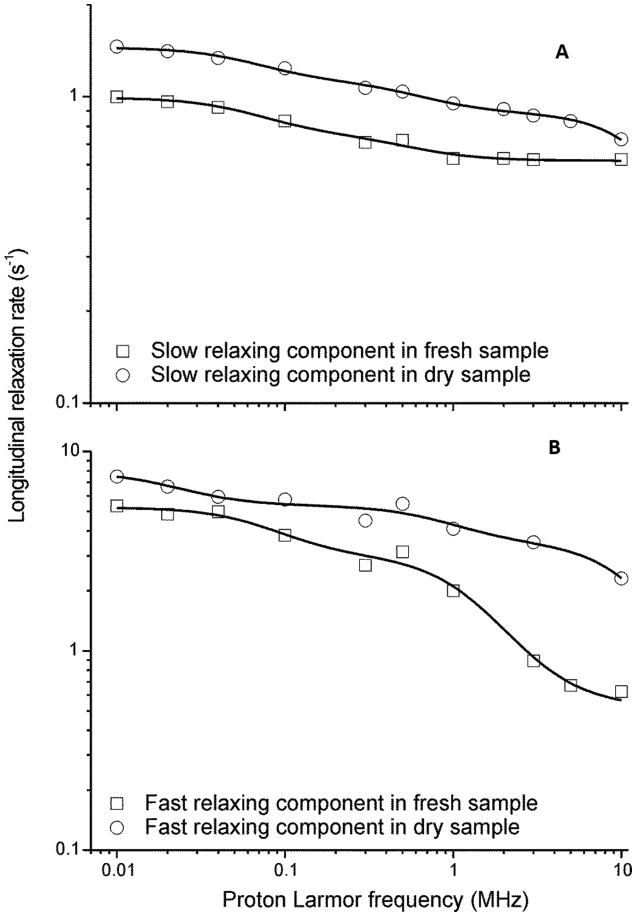

Figure 5. NMRD profiles of the slow relaxing components (A) and fast relaxing components (B) of the fresh and dried *A. donax* L. sample.

Wettability is considered as the ability of a liquid to maintain contact with a solid surface, as a result of the intermolecular interactions when the liquid is brought in contact with the solid surface. For this reason, according to the qualitative evaluation of the NMRD profiles in Figure 5, we suggest that the wettability of the dry fibers is higher than that of the fresh ones.

The larger wettability of the plant fibers following desiccation and rehydration prior of the NMRD experiments explains the larger bending properties, which are reported in the discussion above. In fact, the presence of strongly bound water after dessication and rehydration makes the giant reeds fibers more flexible, thereby allowing a larger resistance to mechanical stresses.

The qualitative evaluation of the NMRD profiles in Figure 5 was confirmed by the quantitative assessment retrieved by the application of the model-free analysis reported in Halle et al.[28] In fact, application of the aforementioned model (see Section 4) returns correlation time (τ_C) values (Figure 6), which can be roughly defined as the time taken for a molecule to rotate 1 rad or to move a distance of the order of its own dimension.[45] The longer the τ_C value, the slower are the molecular motions, thereby revealing restrictions in the motional freedom degrees of spatially restrained molecular systems. Conversely, as a molecule encompasses faster motions due to higher degrees of freedom in larger spaces, shorter correlation time values are expected.

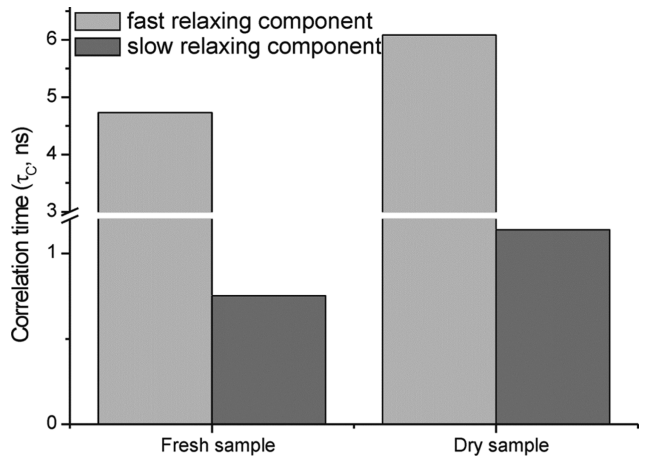

Figure 6. Correlation times, retrieved as reported in Section 4, for the slow and fast components of the fresh and dried *A. donax* L. sample.

Figure 6 shows that water molecules interacting with the surface of the fresh plant sample move faster than those on the surface of the dry *A. donax* L., thereby revealing that the surface interactions on the fresh fibers are weaker than those on the dry ones.

3. CONCLUSIONS

This study reports for the first time the evaluation of the bending stiffness of giant reed *A. donax* L. as affected by the treatment conditions by combining different mechanical and chemical−physical methodologies.

DOI: 10.1021/acsomega.8b02649
ACS Omega 2018, 3, 18510−18517

The mechanical results revealed that it is possible to obtain a wide range of bending stiffness of giant reed by varying the treatment conditions, thereby making it a viable material in several structural applications. In particular, as a function of the treatment conditions investigated in this study, the bending modulus of the samples with node ranges between 2.42 and 7.15 GPa, the bending strength between 26.4 and 83.1 MPa, whereas the deformation at break between 0.82 and 2.86%. For what concerns the samples without node, the bending modulus ranges between 0.96 and 3.26 GPa, the bending strength between 12.2 and 38.2 MPa, whereas the deformation at break between 1.80 and 3.92%. For this reason, the influence of the treatment conditions on the bending stiffness of giant reed is found to be greater for the samples with node than for the samples without node.

It is worth noting that, regardless of the presence of the node, the improvement of the bending modulus can be attributed to the decrease of the moisture content below the fiber saturation point of the giant reed. The latter conclusion has been also verified by DSC analysis. In fact, DSC confirmed that the nodes contain more water than the internodes due to a larger amorphous cellulose fraction. Moreover, the heats of dehydration up to 1500 h from the beginning of the treatment are due to bound water. The latter is the only type of water remaining in the giant reed when the moisture content decreases below the fiber saturation point. Finally, the NMRD results revealed a larger wettability of the dried fibers, thereby confirming that the enhancement of the bending properties after controlled drying are due to a better interaction between water and *A. donax* L. fibers.

4. MATERIAL AND METHODS

Reeds provided by a local trading company were used as a control. These reeds have been dried through a natural drying treatment consisting of two different steps. Immediately after the collection (at the end of winter, usually during the last days of February), the reeds are placed upright leaning against a wall for a period of 1 month. That way, the moisture slowly drains to the bottom part of the reeds and is discarded. Afterward, the reeds are left outside to dry under the direct sunlight at least for a period of 4 months.

A second set of giant reeds was freshly collected in a plantation in the area of Altavilla Milicia (Sicily, Italy). The plants from this second set were divided in two aliquots. A first aliquot was immediately used to evaluate the bending properties and moisture content of the native wet reeds. The second aliquot was dried in a Binder climatic chamber under humidity−temperature-controlled conditions (i.e., at 30 ± 2 °C and 50 ± 5% relative humidity). The latter is also referred to as RH and periodically removed within the range 0−2000 h. After the aforementioned treatment, part of the giant reeds was also oven-dried at 103 ± 2 °C for 24 h to investigate the properties of the completed dried reeds (i.e., moisture-free).

The high water-soluble extractive content in *A. donax* L. (mainly consisting of glucose, fructose, and sucrose) may influence the viscoelastic behavior such as mechanical relaxation.[25,26]

To evaluate the influence of the water-soluble extractive content on the static bending properties of giant reed, two sets of fully dried samples were re-moistened and analyzed. In particular, the first set was soaked in distilled water at room temperature for 4 days to remove the water-soluble material and the second one was soaked in 5% glucose solution for 4 days, as suggested by Obataya and Norimoto.[26] Concerning the sugar content, it is possible to account for the values reported in Obataya and Norimoto:[26] 0% for the samples re-moistened in distilled water, 18.3% for samples re-moistened in glucose solution, and 14% for all the remaining samples.

4.1. Moisture Content. The moisture content (MC) of all the samples was measured by the following relationship

$$\mathrm{MC} = \frac{m_t - m_d}{m_d} \times 100$$

here, m_t is the weight of the samples in the condition analyzed (either naturally dried, controlled dried, or re-moistened) and m_d is the oven-dried and moisture-free weight of the samples.

4.2. Bending Characterization. Three point bending tests (Figure 1) were performed using an Universal Testing Machine (UTM) mod. Z-005 by Zwick-Roell, equipped with a load cell of 5 kN, to evaluate the flexural properties of giant reed. The span length was set equal to 150 mm and cross-head speed to 1 mm/min.

Each treatment condition was investigated by testing 14 samples with length of 200 mm (7 samples were with node, whereas the remaining 7 were without node). A total of 11 sets (i.e., 154 samples, 77 with node and 77 without) were mechanically tested, as reported in Table 1.

To minimize the effect of the dimensional inhomogeneity of the reeds on their mechanical behavior, all the samples were derived from the culms between the fifth and the eighth node above the roots. Six measurements of outer and inner diameter were carried out per sample (two per each end and two in the middle zone), hence these six measured values were mediated.

4.3. Differential Scanning Calorimetry (DSC). DSC curves of giant reeds were recorded by using a differential scanning calorimeter by Shimadzu, model DSC-60. Samples of approximately 5−10 mg were used in sealed aluminum pans.

Aim of this analysis was to evaluate the heat of dehydration of giant reed in the different conditions analyzed (e.g., naturally dried, controlled dried, and re-moistened). For this reason, experiments were performed on samples obtained both from nodes and from internodes.

All tests were carried out in temperature ramp mode with scanning temperature of 5 °C min^{-1} ranging from room temperature up to 200 °C under nitrogen atmosphere (N_2 flow of 50 mL min^{-1}).

4.4. Fast Field Cycling ^{1}H Nuclear Magnetic Resonance Relaxometry (FFC NMR). The theory of fast field cycling (FFC) NMR relaxometry has been reported in other papers.[27] For this reason, only the experimental setup used to analyze *A. donax* L. suspended in water is reported in the present study.

A. donax L. was collected and grinded. An aliquot was directly analyzed by ^{1}H FFC NMR relaxometry, whereas a second aliquot was first overnight dried in oven at 40 °C and then analyzed by FFC NMR technique. Before the NMR analyses, either the fresh or the dried material (around 1 g) was suspended in 3 mL Milli Q grade water (resistivity 18.2 Ω, Merck-Millipore Simplicity 185, Milan, Italy).

^{1}H NMR dispersion (NMRD) profiles (i.e., relaxation rates R_1 or $1/T_1$ vs proton Larmor frequencies, ω_L) were acquired on a Stelar Smartracer Fast-Field-Cycling Relaxometer (Stelar s.r.l., Mede, PV—Italy) at a constant temperature (25 °C). The proton spins were polarized at a polarization field (B_{POL}) corresponding to a proton Larmor frequency (ω_L) of 8 MHz for a period of polarization (T_{POL}) corresponding to about 5

DOI: 10.1021/acsomega.8b02649
ACS Omega 2018, 3, 18510−18517

times the T_1 estimated at this frequency. After each B_{POL} application, the magnetic field intensity (indicated as B_{RLX}) was systematically changed in the proton Larmor frequency ω_L comprised in the range 0.01−10.0 MHz. The period τ, during which B_{RLX} was applied, has been varied on 32 logarithmic spaced time sets. Eight scans were set and the $T_{1,max}$, T_{POL}, and recycle delay were adjusted at every relaxation field to optimize the sampling of the decay/recovery curves.

Free induction decays were recorded following a single ^{1}H 90° pulse applied at an acquisition field (B_{ACQ}) corresponding to the proton Larmor frequency of 7.20 MHz. A time domain of 100 μs sampled with 512 points was applied. Field-switching time was 3 ms, whereas spectrometer dead time was 15 μs. A nonpolarized FFC sequence was applied when the relaxation magnetic fields were in the range of the proton Larmor frequencies between 10.0 and 3.6 MHz, whereas a polarized FFC sequence was applied in the proton Larmor frequencies B_{RLX} in the range of 3.0−0.01 MHz (Kimmich and Anoardo,[29] 2004).

4.4.1. FFC NMR Relaxometry Data Elaboration. The decay/recovery curves acquired as previously described showed a biexponential behavior. To obtain two different longitudinal relaxation times, eq 1 was applied for the decay curves, whereas eq 2 was used for the recovery curves[27]

$$M(\tau) = a + \sum_{i=1}^{N} b_i \exp\left\{-\frac{\tau}{T_{1i}}\right\} \quad (1)$$

$$M(\tau) = a + \sum_{i=1}^{N} b_i\left(1 - \exp\left\{-\frac{\tau}{T_{1i}}\right\}\right) = \left(a + \sum_{i=1}^{N} b_i\right) - \sum_{i=1}^{N} b_i \exp\left\{-\frac{\tau}{T_{1i}}\right\} \quad (2)$$

here, a is the offset, b_i is the magnetization intensity at the Boltzmann equilibrium of the ith component of the molecular motion at each fixed B_{RLX} intensity, τ is the period of time during which B_{RLX} was applied, and N = 2. The two T_1 components provide the longitudinal relaxation rates ($R_1 = 1/T_1$) for the free moving water at each proton Larmor frequency (the slowest R_1 component reported in Figure 1A) and for the water molecules directly interacting with the biomass surface (the fastest R_1 component in Figure 1B).

The NMRD profiles reporting the calculated R_1 values vs Larmor angular frequency (ω_L) were fitted in OriginPro 7.5 SR6 by using the model-free-analysis proposed by Halle et al.[28]

$$R_1 = \frac{\sum_{i=1}^{N} C_i \frac{\tau_{C_i}}{1 + (\omega_L \tau_{C_i})^2}}{\sum_{n=1}^{N} C_i} \quad (3)$$

In the aforementioned equation, R_1 is the longitudinal relaxation rate; τ_{C_i} is the ith correlation time, a typical parameter for spectral density, which, in turn, describes random molecular motions;[29] and C_n is a constant.

AUTHOR INFORMATION

Corresponding Author

*E-mail: pellegrino.conte@unipa.it. Phone: +39 09123864673. Fax: +39 091484035.

ORCID

Pellegrino Conte: 0000-0002-2211-1225

Notes

The authors declare no competing financial interest.

ACKNOWLEDGMENTS

All the authors equally contributed to the project realization.

REFERENCES

(1) Perdue, R. E. *Arundo donax* - source of musical reeds and industrial cellulose. *Econ. Bot.* **1958**, *12*, 368−404.

(2) Ververis, C.; Georghiou, K.; Christodoulakis, N.; Santas, P.; Santas, R. Fiber dimensions, lignin and cellulose content of various plant materials and their suitability for paper production. *Ind. Crops Prod.* **2004**, *19*, 245−254.

(3) Shatalov, A. A.; Pereira, H. Papermaking fibers from giant reed (*Arundo donax* L.) by advanced ecologically friendly pulping and bleaching technologies. *BioResources* **2006**, *1*, 45−61 http://ojs.cnr.ncsu.edu/index.php/BioRes/article/view/BioRes_01_1_045_061_Shatalov_P_Giant_Reed_Fibers/124 .

(4) Al-Snafi, A. E. The constituents and biological effects of *Arundo donax* - a review. *Int. J. Phytopharm. Res.* **2015**, *6*, 34−40.

(5) Fiore, V.; Scalici, T.; Valenza, A. Characterization of a new natural fiber from *Arundo donax* L. as potential reinforcement of polymer composites. *Carbohydr. Polym.* **2014**, *106*, 77−83.

(6) Faix, O.; Meier, D.; Beinhoff, O. Analysis of lignocelluloses and lignin from *Arundo donax* L. and *Miscanthus sinensis* Anderss., and hydroliquefaction of *Miscanthus*. *Biomass* **1989**, *18*, 109−126.

(7) Corno, L.; Pilu, R.; Adani, F. *Arundo donax* L.: A non-food crop for bioenergy and bio-compound production. *Biotechnol. Adv.* **2014**, *32*, 1535−1549.

(8) Lemons e Silva, C. F.; Artigas Schirmer, M.; Nobuyuki Maeda, R.; Araújo Barcelos, C.; Pereira, N., Jr. Potential of giant reed (*Arundo donax* L.) for second generation ethanol production. *Electron. J. Biotechnol.* **2015**, *18*, 10−15.

(9) Garcia-Ortuno, T.; Andreu-Rodriguez, J.; Ferrandez-Garcia, T.; Ferrandez-Villena, M.; Ferrandez-Garcia, C. E. Evaluation of the physical and mechanical properties of particleboards made from giant reed (*Arundo donax* L.). *BioRes* **2011**, *6*, 477−486 http://ojs.cnr.ncsu.edu/index.php/BioRes/article/view/BioRes_06_1_0477_GarciaO_AFFF_Eval_Particalboard_Giant_Reed_Arundo_D/826 .

(10) Flores, J. A.; Pastor, J. J.; Martinez-Gabaroon, A.; Gimeno-Blanes, F. J.; Rodriguez-Guisado, I.; Frutos, M. J. *Arundo donax* chipboard based on urea-formaldehyde resin using under 4 mm particles size meets the standard criteria for indoor use. *Ind. Crops Prod.* **2011**, *34*, 1538−1542.

(11) Fiore, V.; Botta, L.; Scaffaro, R.; Valenza, A.; Pirrotta, A. PLA based biocomposites reinforced with *Arundo donax* fillers. *Compos. Sci. Technol.* **2014**, *105*, 110−117.

(12) Fiore, V.; Scalici, T.; Vitale, G.; Valenza, A. Static and dynamic mechanical properties of *Arundo donax* fillers-epoxy. *Mater. Des.* **2014**, *57*, 456−464.

(13) Ismail, Z. Z.; Jaeel, A. J. A novel use of undesirable wild giant reed biomass to replace aggregate in concrete. *Constr. Build. Mater.* **2014**, *67*, 68−73.

(14) Pilu, R.; Bucci, A.; Badone, F.; Landoni, M. Giant reed (*Arundo donax* L.): A weed plant or a promising energy crop? *Afr. J. Biotechnol.* **2012**, *11*, 9163−9174.

(15) Barreca, F. Use of giant reed *Arundo Donax* L. in rural constructions. *Agric. Eng Int: CIGR J.* **2012**, *14*, 46−52 http://www.cigrjournal.org/index.php/Ejounral/article/view/2076 .

(16) Niklas, K. J. Modes of mechanical failure of hollow, septate stems. *Ann. Bot.* **1998**, *81*, 11−21.

(17) Spatz, H. C.; Boomgaarden, C.; Speck, T. Contribution to the biomechanics of the plants. 3. Experimental and theoretical-studies of local buckling. *Bot. Act.* **1993**, *106*, 254−264.

(18) Shatalov, A. A.; Pereira, H. Influence of stem morphology on pulp and paper properties of *Arundo donax* L. reed. *Ind. Crops Prod.* **2002**, *15*, 77−83.

DOI: 10.1021/acsomega.8b02649
ACS Omega 2018, 3, 18510−18517

(19) Spatz, H. C.; Beismann, H.; Brucher, F.; Emanns, A.; Speck, T. Biomechanics of the giant reed *Arundo donax*. *Philos. Trans. R. Soc., B* **1997**, *352*, 1−10.
(20) Rüggeberg, M.; Burgert, I.; Speck, T. Structural and mechanical design of tissue interfaces in the giant reed *Arundo donax*. *J. R. Soc., Interface* **2010**, *7*, 499−506.
(21) Lord, A. E., Jr. Viscoelasticity of the giant reed material *Arundo donax*. *Wood Sci. Technol.* **2003**, *37*, 177−188.
(22) Speck, O.; Spatz, H. C. Damped oscillations of the giant reed *Arundo donax* (Poaceae). *Am. J. Bot.* **2004**, *91*, 789−796.
(23) Obataya, E.; Gril, J.; Thibaut, B. Shrinkage of cane (*Arundo donax*) I. Irregular shrinkage of green cane due to the collapse of parenchyma cells. *J. Wood Sci.* **2004**, *50*, 295−300.
(24) Obataya, E.; Gril, J.; Perrè, P. Shrinkage of cane (*Arundo donax*) II. Effects of drying condition on the intensity of cell collapse. *J. Wood Sci.* **2005**, *51*, 130−135.
(25) Obataya, E.; Umezawa, T.; Nakatsubo, F.; Norimoto, M. The effects of water soluble extractives on the acoustic properties of reed (*Arundo donax* L.). *Holzforschung* **1999**, *53*, 63−67.
(26) Obataya, E.; Norimoto, M. Mechanical relaxation processes due to sugars in cane (*Arundo donax* L.). *J. Wood Sci.* **1999**, *45*, 378−383.
(27) Conte, P. Environmental Applications of Fast Field Cycling NMR. In *Field Cycling NMR: Instrumentation, Model Theories and Applications*, 1st ed.; Kimmich, R., Ed.; The Royal Society of Chemistry, 2019; pp 229−254.
(28) Halle, B.; Johannesson, H.; Venu, K. Model-Free Analysis of stretched relaxation dispersions. *J. Magn. Reson.* **1998**, *135*, 1−13.
(29) Kimmich, R.; Anoardo, E. Field-cycling NMR relaxometry. *Prog. Nucl. Magn. Reson. Spectrosc.* **2004**, *44*, 257−320.
(30) Niklas, K. J. Responses of hollow, septate culms to vibrations: Biomechanical evidence that nodes can act mechanically as spring-like joints. *Ann. Bot.* **1997**, *80*, 437−448.
(31) Gerhards, C. C. Effect of moisture content and temperature on the mechanical properties of wood: an analysis of the immediate effects. *Wood Fiber Sci.* **1982**, *14*, 4−36 https://wfs.swst.org/index.php/wfs/article/viewFile/501/501 .
(32) Green, D. W.; Link, C. L.; DeBonis, A. L.; McLain, T. E. Predicting the effect of moisture content on the flexural properties of southern pine dimension lumber. *Wood Fiber Sci.* **1986**, *18*, 134−156 https://www.fpl.fs.fed.us/documnts/pdf1986/green86a.pdf .
(33) Wang, S. Y.; Wang, H. L. Effects of moisture content and specific gravity on static bending properties and hardness of six wood species. *J. Wood Sci.* **1999**, *45*, 127−133.
(34) Ishimaru, Y.; Arai, K.; Mizutani, M.; Oshima, K.; Iida, I. Physical and mechanical properties of wood after moisture conditioning. *J. Wood Sci.* **2001**, *47*, 185−191.
(35) Müller, U.; Joscak, T.; Teischinger, A. Strength of dried and re-moistened spruce wood compared to native wood. *Holz Roh- Werkst.* **2003**, *61*, 439−443.
(36) Hailwood, A. J.; Horrobin, S. Absorption of water by polymers: Analysis in terms of a simple model. *Trans. Faraday Soc.* **1946**, *42*, B084−B102.
(37) Barreto, A. C. H.; Rosa, D. S.; Fechine, P. B. A.; Mazzetto, S. E. Properties of sisal fibers treated by alkali solution and their application into cardanol-based biocomposites. *Composites, Part A* **2011**, *42*, 492−500.
(38) Silva, G. G.; Souza, D. A.; Machado, J. C.; Hourston, D. J. Mechanical and thermal characterization of native Brazilian coir fiber. *J. Appl. Polym. Sci.* **2000**, *76*, 1197−1206.
(39) Shukla, S. R.; Athalye, A. R. Mechanical and thermal properties of glycidyl methacrylate grafted cotton cellulose. *J. Appl. Polym. Sci.* **1995**, *57*, 983−988.
(40) Chen, H. Chemical Composition and Structure of Natural Lignocellulose. In *Biotechnology of Lignocellulose: Theory and Practice*; Chen, H., Ed.; Chemical Industry Press: Beijing and Springer Science +Business Media Dordrecht, 2014; pp 25−71.
(41) Neto, C. P.; Seca, A.; Nunes, A. M.; Coimbra, M. A.; Domingues, F.; Evtuguin, D.; Silvestre, A.; Cavaleiro, J. A. S. Variations in chemical composition and structure of macromolecular components in different morphological regions and maturity stages of *Arundo donax*. *Ind. Crops Prod.* **1997**, *6*, 51−58.
(42) Ciolacu, D.; Ciolacu, F.; Popa, V. I. Amorphous cellulose-structure and characterization. *Cellul. Chem. Technol.* **2011**, *45*, 13−21 http://www.cellulosechemtechnol.ro/pdf/CCT1-2(2011)/p.13-21.pdf .
(43) Callaghan, P. T.; Coy, A. PGSE NMR and Molecular Translational Motion in Porous Media. In *Nuclear Magnetic Resonance Probes of Molecular Dynamics*; Tycho, R., Ed.; Kluwer Academic Publishers: Dordrecht, 1994; pp 489−523.
(44) Conte, P.; Marsala, V.; De Pasquale, C.; Bubici, S.; Valagussa, M.; Pozzi, A.; Alonzo, G. Nature of water-biochar interface interactions. *GCB Bioenergy* **2013**, *5*, 116−121.
(45) Bakhmutov, V. I. *Practical NMR Relaxation for Chemists*; Wiley: Chichester, 2004.

DOI: 10.1021/acsomega.8b02649
ACS Omega 2018, 3, 18510−18517